Inorganic Chemistry

Article

pubs.acs.org/IC

Phosphorescence Imaging of Living Cells with Amino Acid-Functionalized Tris(2-phenylpyridine)iridium(III) Complexes

Peter Steunenberg,[†] Albert Ruggi,[†] Nynke S. van den Berg,[‡] Tessa Buckle,[‡] Joeri Kuil,[‡] Fijs W.B. van Leeuwen,[‡] and Aldrik H. Velders*[,†,§]

[†]Supramolecular Chemistry and Technology, MESA+ Institute for Nanotechnology, University of Twente, P.O. Box 217, 7500 AE, Enschede, The Netherlands

[‡]Division of Diagnostic Oncology, The Netherlands Cancer Institute, Plesmanlaan 121, 1066 CX, Amsterdam, The Netherlands; Interventional Molecular Imaging Section, Department of Radiology, Leiden University Medical Center, Leiden, The Netherlands

[§]BioNanoTechnology group, Laboratory of Physical Chemistry and Colloid Science Wageningen University, Dreijenplein 6, 6703 HB, Wageningen, The Netherlands

S *Supporting Information*

ABSTRACT: A series of nine luminescent cyclometalated octahedral iridium(III) tris(2-phenylpyridine) complexes has been synthesized, functionalized with three different amino acids (glycine, alanine, and lysine), on one, two, or all three of the phenylpyridine ligands. All starting complexes and final compounds have been fully analyzed by one-dimensional (1D) and two-dimensional (2D) NMR spectroscopy, and photophysical data have been obtained for all the mono-, bis-, and tri- substituted iridium(III) complexes. Cellular uptake and localization have been studied with flow cytometry and confocal microscopy, respectively. Confocal experiments demonstrate that all nine substituted iridium(III) complexes show variable uptake in the tumor cells. The monosubstituted iridium(III) complexes give the highest cellular uptake, and the series substituted with lysines shows the highest toxicity. This systematic study of amino acid-functionalized $Ir(ppy)_3$ complexes provides guidelines for further functionalization and possible implementation of luminescent iridium complexes, for example, in (automated) peptide synthesis or biomarker specific targeting.

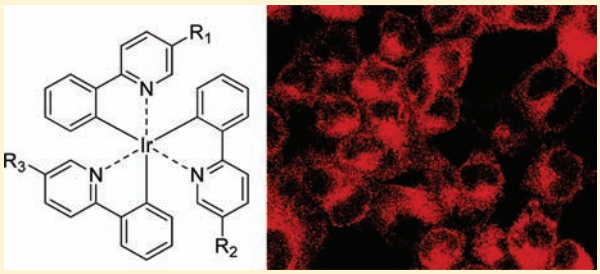

INTRODUCTION

Luminescent complexes with lanthanide ions or late first-row transition metal ions, for example, zinc or copper,[1,2] have been applied in optical imaging already for a while, but only more recently d^6 transition metal complexes have proven their potential as luminophores in fluorescence cell microscopy.[3] Luminescence based imaging is one of the most convenient ways to study cells as it visualizes morphological details with subcellular resolution which cannot be achieved by other imaging modalities.[4−6] Organic fluorophores still constitute the class of the most used fluorescent probes,[7] but they have limitations such as easy photobleaching, small Stokes shifts, and the same (short) fluorescent lifetime as the autofluorescence observed in organisms/tissues.[8] Iridium(III) complexes exhibit a high luminescent quantum yield (0.5−1.0 in most degassed organic solvents and still about 0.1 in aqueous solutions), have a tunable luminescent color (from blue to red), and relatively long lifetimes, which may yield favorable properties in imaging applications.[9] These properties have resulted in their utilization in organic light-emiting diodes,[10] phosphorescent chemosensing systems,[11] light-emiting electrochemical cells,[12] luminescence sensitizers,[13] and pressure sensitive paints (aerodynamic applications).[14] First studies on applications of iridium for diagnostic imaging have been performed by Lo et al.,[15] and Li et al.,[16] using cationic iridium(III) complexes with neutral bidentate, for example, 2,2′-bipyridine (bpy), ligands. Although these complexes show good cellular uptake,[17] low toxicity, reduced photobleaching, and exclusive staining of the cytoplasm, these cationic dyes still suffer from a significantly lower quantum yield compared with the neutral fully cyclometalated complexes: 0.4 for $Ir(ppy)_3$ vs 0.06 for $[(ppy)_2Ir(bpy)](PF_6)$ (in degassed dichloromethane solutions).[18] Some cationic iridium(III) complexes show even lower quantum yields (CH_3CN 0.017, MeOH 0.0064 and PBS/MeOH 9:1 even 0.0021); the values obtained for neutral complexes show at least a 10-fold improvement compared to those values.[19]

Here we report on the cellular uptake and localization of nine neutral iridium(III) complexes with fully cyclometalated neutral tris(2-phenylpyridine) cores. The archetypical octahedral $Ir(ppy)_3$ itself is poorly soluble in aqueous media,[20] and Li et al. briefly described the troublesome cellular uptake of neutral iridium(III) complexes.[21] However, upon introduction of one,

Received: August 25, 2011
Published: February 3, 2012

two, or three ppy ligands conjugated to three different amino acids, an improved water solubility is observed; the quantum yields of the luminescence (0.1−0.15) further allows good conditions for comparison of their cellular uptake, distribution, and (bio)imaging properties. The use of cationic iridium(III) complexes, as described before,[15,16] is well established, but the higher stability of neutral iridium(III) complexes, allowing a wider range of synthetic modifications, together with the small improvements of the photophysical properties, can already mean a major advantage. The cellular uptake is significantly influenced by the number and type of substituents, yielding initial guidelines for the design of new biolabels.

EXPERIMENTAL SECTION

^{1}H NMR (600 MHz) and ^{13}C NMR (151 MHz) data were obtained using a Bruker Avance II NMR-spectrometer. All spectra are referenced to residual proton solvent signal. Abbreviations used include singlet (s), doublet (d), doublet of doublets (dd), triplet (t), and unresolved multiplet (m). ^{13}C NMR assignments were made by analyzing the HC-HMBC, HC-HMQC, and HH−COSY spectra. Mass spectral data were obtained using an Applied Biosystems Voyager DE-RP MALDI-TOF Spectrometer. HRMS analyses were obtained using a Waters/Micromass LCT mass spectrometer. Emission measurements were acquired using a Perkin-Elmer Fluorescence spectrometer. IR-spectra were recorded using a Thermo Scientific Nicolet TM 6700 FT-IR spectrometer equipped with a Smart Orbit diamond ATR accessory. Abbreviations used include (w) weak, (m) medium, (s) strong, and (vs) very strong. UV−vis spectra were measured on a Perkin-Elmer Lambda 850 UV−vis spectrophotometer. Steady-state luminescence spectra were measured using an Edinburgh FS900 fluorospectrometer. A 450 W xenon arc lamp was used as excitation source. Luminescence quantum yields at room temperature (Φ and Φ_{air}) were evaluated by comparing wavelength-integrated intensities (I and I_R) of isoabsorptive optically diluted solutions (Abs <0.1) with reference to $[Ru(bpy)_3]Cl_2$ (Φ_R = 0.028 in air-equilibrated water) standard and by using the eq 1

$$\Phi = \Phi_R \frac{n^2 I}{n_R^2 I_R} \quad (1)$$

where n and n_R are the refractive index of the sample and reference solvent, respectively.[22]

Materials and Reagents. $IrCl_3 \cdot 4H_2O$ and 2-phenylpyridine were purchased from ABCR. Phenylboronic acid, 6-bromo-pyridine-3-carboxylic acid, and the amino acids (glycine, alanine, and lysine) were acquired from Sigma Aldrich, and tetrakis(triphenylphosphino)-palladium from Acros. All other reagents and solvents were purchased from VWR. All commercial materials were used without further purification. The dimeric complex $[(ppy)_2Ir(\mu\text{-}Cl)_2Ir(ppy)_2]$ (**1**) was synthesized as previously reported.[23]

Methyl 2-Phenyl-5-carboxypyridine (mppy) (2). A mixture of phenylboronic acid (1.6 g, 14 mmol), 6-bromo-pyridine-3-carboxylic acid (2.0 g 10 mmol), tetrahydrofuran (THF, 50 mL), water (50 mL), and Na_2CO_3 (1M, 50 mL) was stirred under argon; then tetrakis(triphenylphosphino)palladium (250 mg, 0.25 mmol) was added in one portion. The yellow solution was stirred for 24 h at 100 °C. Afterward the THF was removed, and the remaining aqueous phase was extracted with dichloromethane (3 times 50 mL). The aqueous phase was then acidified by conc. HCl and 2-phenyl-5-carboxypyridine precipitated. The compound was isolated by filtration and dried under vacuum over P_2O_5. 2-Phenyl-5-carboxypyridine was obtained in 1.8 g (90%) as a white solid. This product was used in the next step without further purification. 2-Phenyl-5-carboxypyridine (2 g, 10 mmol) was refluxed overnight in MeOH (70 mL) and H_2SO_4 (4 mL). After evaporation of the solvent, water (100 mL) was added, and the mixture was neutralized with saturated $NaHCO_3$ solution. The aqueous phase was then extracted with diethylether (2 times 100 mL). The combined organic fractions were washed with water (100 mL), brine (50 mL), and dried over $MgSO_4$. Upon evaporation of the solvent the compound was obtained in a 90% yield (1.8 g, 9 mmol) as a white solid. ^{1}H NMR in accordance with literature.[24,25]

***fac*-(ppy)$_2$(mppy)Ir (4) and *fac*-(ppy)(mppy)$_2$Ir (5).** $[(ppy)_2Ir(\mu\text{-}Cl)_2Ir(ppy)_2]$ (**1**) (200 mg, 0.2 mmol), mppy (**2**) (200 mg, 0.9 mmol), $AgCF_3SO_3$ (100 mg, 0.4 mmol), and toluene (15 mL) were placed in a reaction vessel and degassed. The reaction mixture was heated at 120 °C while under continuous stirring for 5 h. The resulting dark orange-red solution was cooled to room temperature and directly transferred to a silica column. The product was eluted with CH_2Cl_2. The monosubstituted product **4** (45 mg, 0.06 mmol, 15%) was found in the first fractions, the bis-substituted product **5** (65 mg, 0.09 mmol, 22%) in the middle fractions.[26] ***fac*-(ppy)$_2$(mppy)Ir (4):** ^{1}H NMR (DMSO) δ 3.72 (s, 3H, MeO), 6.6−6.8 (m, 6H, H-Ph6, H-Ph5, H-Ph6′,H-Ph5′), 6.8−6.9 (m, 3H, H-Ph4, H-Ph4′), 7.13, 7.19 (2t, 2H, J = 6.5, H-Py5′), 7.50, 7.55 (2 d, 2H, J = 6.5, H-Py6′), 7.79 (d, 2H, J = 8.0, H-Ph3′), 7.8−7.9 (m, 3H, H-Ph3, H-Py4′), 7.99 (s, 1H, J = 2.0, H-Py6), 8.17 (m, 3H, H-Py3′, H-Py4), 8.26 (d, 1H, J = 8.0, H-Py3), ^{13}C NMR (DMSO) δ 52.6, 118.9, 119.7, 120.4, 123.4, 124.2, 124.8, 126.3, 129.5, 130.6, 136.6, 137.5, 137.9, 142.9, 144.2, 147.6, 148.5, 160.3, 164.0, 164.9, 165.8, 170.1, IR (neat) 3035 (w), 1711 (s), 1598 (s), 1578 (s), 1471 (s), 1290 (m), 1126 (m), 747 (vs), 734 (vs) cm^{-1}, MALDI-TOF MS (dithranol) $[M]^+$ Calcd. for: 713, Found: 713, HRMS (ESI-MS) Calcd. for: $C_{35}H_{27}IrN_3O_2$ $[M]^+$, 713.1656 Found: 713.1598. ***fac*-(ppy)(mppy)$_2$Ir (5):** ^{1}H NMR (DMSO) δ 3.72, 3.74 (2 s, 6H, MeO), 6.6−6.8 (m, 9H, H-Ph6,5,4,6′,5′,4′), 7.17 (t, 1H, J = 6.0, H-Py5′), 7.60 (d, 1H, J = 6.0, H-Py6′), 7.80 (d, 1H, J = 8.0, H-Ph3′), 7.88 (m, 3H, H-Ph3, H-Py4′), 7.97, 8.00 (2 d, 2H, J = 2.0, H-Py6), 8.24 (m, 3H, H-Py3′, H-Py4), 8.26, 8.31 (2 d, 2H, J = 8.0, H-Py3), ^{13}C NMR (DMSO) δ 52.3, 118.9, 119.8, 120.2, 123.1, 124.1, 124.6, 126.4, 129.6, 136.5, 137.4, 137.8, 142.8, 144.3, 147.9, 148.5, 160.5, 163.9, 165.5, 165.7, 169.7, IR (neat) 3044 (w), 1715 (s), 1544 (s), 1288 (m), 1252 (m), 1124 (m), 743 (vs), 730 (vs) cm^{-1}, MALDI-TOF MS (dithranol) m/z $[M+H]^+$ Calcd. for: 772, Found: 772, HRMS (ESI-MS), Calcd. for: $C_{37}H_{28}IrN_3O_4$ $[M]^+$ 771.1709, Found: 771.1707.

Tetrakis(2-phenyl-5-methoxycarbonyl-pyridine-C^2,N′)(μ-dichloro)diiridium(III) (6). Iridium(III) trichloride hydrate (400 mg, 1.1 mmol) was combined with mppy (**2**) (400 mg, 1.2 mmol), dissolved in 2-ethoxyethanol (30 mL), and refluxed for 24 h (the solution was purged with argon and stirred in the dark). The reaction was cooled to room temperature, diluted with 30 mL water, and the orange precipitate (550 mg, 0.8 mmol, 74%) was collected on a glass filter frit. ^{1}H NMR (CD_2Cl_2) δ 3.86 (s, 12H, MeO), 5.87 (d, 4H, J = 8.0, H-Ph6), 6.71 (t, 4H, J = 8.0, H-Ph5), 6.91 (t, 4H, J = 8.0, H-Ph4), 7.69 (d, 4H, J = 8.0, H-Ph3), 8.03 (d, 4H, J = 9.0, H-Py3), 8.33 (d, 4H, J = 9.0, H-Py4), 9.86 (s, 4H, H-Py6), ^{13}C NMR (DMSO) δ 52.9 (C-MeO), 118.2 (C-Py3), 122.4 (C-Ph4), 124.3 (C-Ph3), 125.6 (C-Py5), 130.4 (C-Ph5), 130.5 (C-Ph6), 138.6 (C-Py4), 142.7 (C-Ph2), 147.1 (C-Ph1), 152.7 (C-Py6), 162.5 (C−COOMe), 172.1 (C-Py2), IR (neat) 2996 (w), 1714 (s), 1604 (s), 1582 (s), 1285 (m), 1254 (m), 1124 (m), 796 (vs) cm^{-1}, MALDI-TOF MS (dithranol) $[M\text{-}Cl]^+$ Calcd. for: 1268, Found: 1268, HRMS (ESI-MS) Calcd. for: $C_{52}H_{40}Cl_2Ir_2N_4O_8$ $[M]^+$ 1304.1482, Found: 1304.1459.

***fac*-(mppy)$_3$Ir (7).** $[(mppy)_2Ir(\mu\text{-}Cl)_2Ir(mppy)_2]$ (**6**) (250 mg, 0.2 mmol), mppy (**2**) (200 mg, 0.9 mmol), $AgCF_3SO_3$ (100 mg, 0.4 mmol), and toluene (15 mL) were placed in a reaction vessel and degassed. The reaction mixture was heated at 120 °C while under continuous stirring for 5 h. The resulting dark orange-red solution was cooled to room temperature and directly transferred to a silica column. The product was eluted with CH_2Cl_2/Aceton 8/2. *fac*-(mppy)$_3$Ir was obtained in a yield of 45% (150 mg, 0.09 mmol). ^{1}H NMR (DMSO) δ 3.72 (s, 9H, MeO), 6.59 (d, 3H, J = 7.5, H-Ph6), 6.70 (t, 3H, J = 7.5, H-Ph5), 6.80 (t, 3H, J = 7.5, H-Ph4), 7.80 (d, 3H, J = 7.5, H-Ph3), 7.90 (d, 3H, J = 2.0, H-Py6), 8.15 (dd, 3H, J = 9.0, J = 2.0, H-Py4), 8.22 (d, 3H, J = 9.0, H-Py3), ^{13}C NMR (DMSO) δ 52.9 (OMe), 118.9 (C-Py4), 121.0 (C-Ph4), 124.1 (C-Py5), 126.9 (C-Py6), 131.2 (C-Ph5), 136.9 (C-Ph6), 138.3 (C-Py3), 142.9 (C-Ph2), 148.5 (C-Py6), 161.9 (C-Ph1), 164.1 (C-PyCOOMe), 170.0 (C-Py2), IR (neat) 3036 (w), 2950 (w), 1720 (s), 1598 (s), 1580 (s), 1430 (m), 1284 (m), 1250 (m), 1125 (m), 747 (vs) cm^{-1}, MALDI-TOF MS (dithranol):

dx.doi.org/10.1021/ic201860s | Inorg. Chem. 2012, 51, 2105−2114

m/z $[M]^+$ Calcd. for: 829, Found: 829 HRMS (ESI-MS), Calcd. for: $C_{39}H_{31}IrN_3O_6$ $[M+H]^+$ 830.1844, Found: 830.1797.

***fac*-(ppy)$_2$(cppy)Ir (8).** The obtained red solid mononuclear iridium complexes **4** (general synthetic route for **9** and **10** as well) (0.1 mmol) from the previous step were dissolved in THF/water (20/20 mL), and LiOH (30 mg) was added. The reaction mixture was heated until 45 °C and stirred at this temperature overnight. Afterwards, the reaction mixture was allowed to cool to room temperature, and THF was removed under reduced pressure. The remaining aqueous solution was acidified by 2 N HCl until precipitation of the product. The red precipitate was isolated by filtration, washed with 20 mL of water and dried. *fac*-(ppy)$_2$(cppy)Ir was obtained in quantitative yield. ^{1}H NMR (DMSO) δ 6.6–6.8 (m, 6H, H-Ph6, H-Ph6′, H-Ph5, H-Ph5′), 6.8–6.9 (m, 3H, H-Ph4, H-Ph4′), 7.14, 7.20 (2 t, 2H, J = 6.5 H-Py5′), 7.50, 7.55 (2d, 2H, J = 6.5, H-Py6′), 7.80 (d, 2H, J = 8.0, H-Ph3′), 7.8–7.9 (m, 3H, H-Ph3, H-Py4′), 7.99 (d, 1H, J = 2.0, H-Py6), 8.15 (m, 3H, H-Py3′, H-Py4), 8.25 (d, 1H, J = 8.0, H-Py3), ^{13}C NMR (DMSO) δ 119.3, 119.4, 120.4, 123.6, 124.7, 126.2, 129.6, 130.5, 136.9, 137.5, 138.1, 143.1, 144.1, 147.4, 149.0, 160.5, 163.8, 166.0, 170.1, IR (neat) 3292 (w), 3036 (w), 1693 (s), 1598 (s), 1259 (m), 750 (vs) cm^{-1}, MALDI-TOF MS (dithranol) $[M]^+$ Calcd. for: 699, Found: 699, HRMS (ESI-MS) Calcd. for: $C_{34}H_{24}IrN_3O_2$, $[M]^+$ 669.1498, Found: 669.1449.

***fac*-(ppy)(cppy)$_2$Ir (9).** This complex was prepared according to the procedure for the synthesis of complex **8** using complex **5** (instead of complex **4**) as the reactant. ^{1}H NMR (DMSO) δ 6.6–6.8 (m, 9H, H-Ph6,6′,5,5′,4,4′), 7.13 (t, 1H, J = 6.0, H-Py5′), 7.54 (d, 1H, J = 6.0, H-Py6′), 7.75 (d, 1H, J = 8.0, H-Ph3′), 7.81 (m, 3H, H-Ph3, H-Py4′), 7.94, 7.99 (2 d, 2H, J = 2.0, H-Py6), 8.22 (m, 3H, H-Py3′, H-Py4), 8.26, 8.31 (2 d, 2H, J = 8.0, H-Py3), ^{13}C NMR (DMSO) δ 119.1, 119.6, 120.4, 123.4, 124.7, 125.5, 126.1, 129.6, 130.9, 136.8, 137.7, 138.2, 143.2, 144.4, 147.8, 148.7, 159.2, 162.9, 163.1, 165.6, 169.3, IR (neat) 3035 (w), 1694 (s), 1579 (s), 1574 (s), 1379 (m), 1223 (m), 749 (vs), 729 (vs) cm^{-1}, MALDI-TOF MS (dithranol): m/z $[M]^+$ Calcd. for: 743, Found 743, HRMS (ESI-MS) Calcd. for: $C_{35}H_{24}IrN_3O_4$ $[M]^+$ 743.1398, Found: 743.1423.

***fac*-(cppy)$_3$Ir (10).** This complex was prepared according to the procedure for the synthesis of complex **8** using complex **7** (instead of complex **4**) as the reactant. ^{1}H NMR (DMSO) δ 6.59 (d, 3H, J = 7.5, H-Ph6), 6.70 (t, 3H, J = 7.5, H-Ph5), 6.80 (t, 3H, J = 7.5, H-Ph4), 7.80 (d, 3H, J = 7.5, H-Ph3), 7.90 (d, 3H, J = 2.0, H-Py6), 8.15 (dd, 3H, J = 9.0, J = 2.0, H-Py4), 8.22 (d, 3H, J= 9.0, H-Py3) ^{13}C NMR (DMSO) δ 119.0 (C-Py4), 120.9 (C-Ph4), 124.3 (C-Py5), 126.4 (C-Py6), 131.1 (C-Ph5), 136.8, (C-Ph6) 138.5 (C-Py3), 143.5 (C-Ph2), 148.9 (C-Py6), 162.1 (C-Ph1), 164.5 (C-PyCOOMe), 169.5 (C-Py2), IR (neat) 3365 (w), 1682 (s), 1597 (s), 1580 (s), 1403 (m), 1226 (m), 749 (vs), 723 (vs) cm^{-1}, MALDI-TOF MS (dithranol): m/z $[M]^+$ Calcd. for: 787, Found: 787 HRMS (ESI-MS), Calcd. for: $C_{36}H_{24}IrN_3O_6$ $[M+H]^+$, 787.1294 Found: 787.1265.

General Procedure for Amino Acid Coupling. The general synthetic route for amino acid conjugated 2-phenylpyridine mononuclear iridium(III) complex conjugated to amino acids is described in Scheme 1. Briefly, 1 equiv of the mononuclear iridium(III) complex (0.06 mmol) was dissolved in dimethylformamide (DMF, 10 mL). To this solution was added DCC (0.18 mmol, i.e., 3 equiv per free acid), HOBt (0.18 mmol or 3 equiv per free acid), amino acid methyl ester (HCl-salt, 0.018 mmol, i.e., 3 equiv per free acid), and DIPEA (0.1 mL), and the reaction mixture was stirred overnight at room temperature. The reaction mixture was concentrated under vacuum, and the crude iridium complex-conjugates were purified by column chromatography (CH_2Cl_2:Aceton 4:1). The so-obtained red solid was dissolved in THF/water (20/20 mL), and LiOH (30 mg per free acid) was added. The reaction mixture was heated until 45 °C and stirred at this temperature overnight. The reaction mixture was cooled to room temperature and acidified to pH 1 by 1.0 M HCl until precipitation of the product. The red precipitate was isolated by filtration, washed with 20 mL water and dried. The amino acid conjugated complexes were obtained as a single product in near quantitative yield.

***fac*-(ppy)$_2$(gly-ppy)Ir (11).** Reactants: glycine methyl ester hydrochloride and complex **8** ^{1}**H NMR** (DMSO) δ 3.84 (m, 2H, CH_2-Gly), 6.6–6.8 (m, 6H, H-Ph6,6′,5,5′), 6.8–6.9 (m, 3H, H-Ph4,4′), 7.15 (t, 2H, J = 6.0, H-Py5′), 7.50, 7.53 (2 d, 2H, J = 6.0, H-Py6′), 7.78 (2d, 2H, J = 8.0, H-Ph3′), 7.80 (m, 2H, H-Py4′), 7.85 (d, 1H, J = 8.0, H-Ph3), 8.04 (s, 1H, H-Py6), 8.16 (2 d, 2H, J = 9.0, H-Py3′), 8.25 (m, 2H, H-Py3,Py4), 9.04 (t, 1H, NH), IR (neat) 3322 (w), 2927 (w), 2849 (w), 1624 (s), 1537 (s), 1309 (m), 1228 (m), 1087 (m), 749 (vs) cm^{-1}, ^{13}C NMR (DMSO) δ 40.9, 118.4, 119.3, 120.1, 123.1, 124.4, 125.6,127.4, 129.3, 130.6, 134.3, 136.8, 137.6, 143.2, 144.0, 147.4, 148.8, 160.8, 163.0, 164.2, 165.9, 166.1, 168.7, 171.8, MALDI-TOF MS (dithranol) Calcd. for: m/z $[M]^+$ 756, Found 756, HRMS (ESI-MS) Calcd. for: $C_{36}H_{27}IrN_4O_3$ $[M]^+$ 756.1712, Found: 756.1667, UV–vis: λ_{abs} 382 nm, λ_{abs} 483 nm, λ_{em} = 579 nm, ε_{382} = 9,096 M^{-1} cm^{-1} ε_{483} = 1,1871 M^{-1} cm^{-1}, Φ 0.12 (in DMSO).

***fac*-(ppy)(gly-ppy)$_2$Ir (12).** Reactants: glycine methyl ester hydrochloride and complex **9** ^{1}H NMR (DMSO) δ 3.83 (dd, 4H, J = 3.8, CH_2-Gly), 6.6–6.8 (m, 6H, H-Ph6,6′,5,5′), 6.8–6.9 (m, 3H, H-Ph4,4′), 7.16 (t, 1H, J = 6.0, H-Py5′), 7.58 (d, 1H, J = 6.0, H-Py6′), 7.77 (d, 1H, J = 8.0, H-Ph3′), 7.83 (t, 1H, J= 6.0, H-Py4′), 7.86 (dd, 2H, J = 8.0, H-Ph3), 8.02 (s, 2H, H-Py6), 8.19 (d, 1H, J = 6.0, H-Py3′), 8.26 (d, 2H, J = 9.0, H-Py4), 8.28 (dd, 2H, J = 9.0, J = 2.0, H-Py3), 9.14 (m, 2H, NH), ^{13}C NMR (DMSO) δ 41.3, 118.5, 119.4, 120.5, 123.9, 124.7, 125.9, 120.9, 135.6, 136.6, 138.2, 143.4, 144.4, 147.9, 148.2, 160.0, 162.6, 165.8, 168.1, 171.4, IR (neat) 3322 (w), 2927 (w), 2849 (w), 1624 (s), 1537 (s), 1309 (m), 1228 (m), 1087 (m), 749 (vs) cm^{-1}, MALDI-TOF MS (dithranol) m/z $[M]^+$ Calcd. for: 857, Found: 857, HRMS (ESI-MS) Calcd. for: $C_{39}H_{31}IrN_5O_6$ $[M+H]^+$ 858.1906, Found: 858.1947, UV–vis: λ_{abs} 401 nm, λ_{abs} 482 nm, λ_{em} = 576 nm, ε_{401} = 7,402 M^{-1} cm^{-1} ε_{482} = 1,858 M^{-1} cm^{-1} Φ 0.13 (in DMSO).

***fac*-(gly-ppy)$_3$Ir (13).** Reactants: glycine methyl ester hydrochloride and complex **10** ^{1}H NMR (DMSO) δ 3.82 (m, 6H, CH_2-Gly), 6.60 (d, 3H, J = 7.5, H-Ph6), 6.72 (t, 3H, J = 7.5, H-Ph5), 6.84 (t, 3H, J = 7.5, H-Ph4), 7.88 (d, 3H, J = 7.5, H-Ph3), 8.05 (s, 3H, H-Py6), 8.30 (m, 6H, H-Py3, H-Py4), 9.16 (t, 3H, J = 5.5, NH), ^{13}C NMR (DMSO) δ 41.2 (C-G1), 118.5 (C-Py4), 120.4 (C-Ph4), 125.7 (C-Ph3), 127.4 (C-Py5), 130.6 (C-Ph5), 135.4 (C-Py3), 136.7 (C-

Scheme 1. Synthesis of Amino Acid Conjugated Complexes 11–19

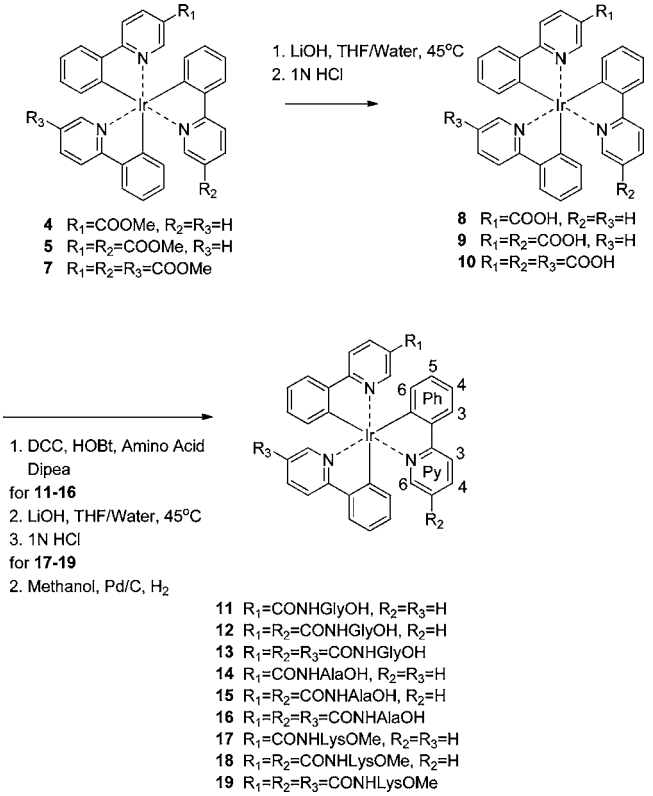

dx.doi.org/10.1021/ic201860s | Inorg. Chem. 2012, 51, 2105–2114

Ph6), 143.0 (C-Ph2), 148.4 (C-Py6), 161.9 (C-Ph1), 163.7 (C-PyCO), 168.5 (C-Py2), 171.6 (C-GCOOH), IR (neat) 3340 (w), 3040 (w), 2928 (w), 1720 (s), 1637 (s), 1594 (s), 1579 (s), 1473 (m), 1299 (m), 1207 (m), 746 (vs), 730 (vs) cm^{-1} MALDI-TOF MS (dithranol) $[M]^+$ Calcd. for: 959, Found: 959, HRMS (ESI-MS) Calcd. for: $C_{42}H_{33}IrN_6O_9$ $[M+H]^+$ 959.2020, Found: 959.2016, UV–vis: λ_{abs} 405 nm, λ_{abs} 485 nm, λ_{em} = 564 nm, ε_{405} = 8,443 M^{-1} cm^{-1} ε_{485} = 2,013 M^{-1} cm^{-1} Φ 0.11 (in DMSO).

***fac*-(ppy)$_2$(ala-ppy)Ir (14).** Reactants: alanine methyl ester hydrochloride and complex **8** ^{1}H NMR (DMSO) δ 1.30 (s, 3H, CH-(CH_3)-COOH) 4.24 (m, 1H, C*H*-(CH_3)-Ala), 6.6–6.8 (m, 6H, H-Ph6,6′,5,5′), 6.8–6.9 (m, 3H, H-Ph4,4′), 7.15 (2t, 2H, *J* = 6.0, H-Py5′), 7.50, 7.53 (2 d, 2H, *J* = 6.0, H-Py6′), 7.75 (2d, 2H, *J* = 8.0, H-Ph3′), 7.81 (m, 2H, H-Py4′), 7.87, (2d, 1H, *J* = 8.0, H-Ph3), 7.98, 8.00 (2d, 1H, *J* = 2.0, H-Py6), 8.15 (m, 2H, H-Py3′) 8.26 (dd, 1H, *J* = 9.0, H-Py4), 8.31, 8.33 (m, 1H, *J* = 9.0, *J* = 2.0, H-Py3), 8.8 (m, 1H, NH), ^{13}C NMR (DMSO) δ 17.5 48.8, 118.5, 119.5, 120.2, 123.4, 124.8, 125.8, 130.6, 135.6, 136.4, 138.1, 143.5, 144.5, 147.9, 159.8, 162.7, 163.4, 165.6, 168.5, 174.8, IR (neat) 3353 (w), 3034 (w), 2924 (w), 1716 (s), 1635 (s), 1597 (s), 1579 (s), 1472 (m), 1256 (m), 1030 (m), 750 (vs), 732 (vs) cm^{-1}, MALDI-TOF MS (dithranol) *m*/*z* $[M+H]^+$ Calcd. for: 771, Found: 771, HRMS (ESI-MS) Calcd. for: $C_{37}H_{29}IrN_4O_3$ $[M]^+$ 770.1869, Found: 771.1795 UV–vis: λ_{abs} 382 nm, λ_{abs} 484 nm, λ_{em} = 579 nm, ε_{382} = 7,152 M^{-1} cm^{-1} ε_{484} = 1,444 M^{-1} cm^{-1} Φ 0.11 (in DMSO).

***fac*-(ppy)(ala-ppy)$_2$Ir (15).** Reactants: alanine methyl ester hydrochloride and complex **9** ^{1}H NMR (DMSO) δ 1.32 (s, 6H, CH-(CH_3)-COOH) 4.24 (m, 2H, C*H*-(CH_3)-Ala), 6.6–6.8 (m, 6H, H-Ph6,6′,5,5′), 6.8–6.9 (m, 3H, H-Ph4,4′), 7.15 (2t, 1H, *J* = 6.0, H-Py5′), 7.55, 7.58 (2 d, 1H, *J* = 6.0, H-Py6′), 7.77 (d, 1H, *J* = 8.0, H-Ph3′), 7.83 (m, 3H, H-Py4′, H-Ph3), 7.98 (m, 2H, H-Py6), 8.15 (m, 1H, H-Py3′) 8.26 (d, 2H, *J* = 9.0, H-Py4), 8.33 (m, 2H, H-Py3) 8.8 (m, 2H, NH), ^{13}C NMR (DMSO) δ 17.4, 48.4, 118.5, 119.7, 120.2, 123.4, 124.8, 125.8, 130.6, 135.6, 136.6, 137.8, 143.5, 144.8, 147.9, 160.2, 162.7, 163.4, 165.6, 168.4, 174.8, IR (neat) 3334 (w), 2929 (w), 1725 (s), 1629 (s), 1580 (s), 1474 (m), 1255 (m), 1029 (m), 1012 (m), 750.6 (vs), 736 (vs) cm^{-1}, MALDI-TOF MS (dithranol) $[M]^+$ Calcd. for: 885, Found: 885 HRMS (ESI-MS) Calcd. for: $C_{41}H_{35}IrN_5O_6$ $[M+H]^+$ 886.2219, Found: 886.2182 UV–vis: λ_{abs} 401 nm, λ_{abs} 483 nm, λ_{em} = 570 nm, ε_{401} = 6,554 M^{-1} cm^{-1} ε_{483} = 2,005 M^{-1} cm^{-1} Φ 0.12 (in DMSO).

***fac*-(ala-ppy)$_3$Ir (16).** Reactants: alanine methyl ester hydrochloride and complex **10** ^{1}H NMR (DMSO) δ 1.30 (s, 9H, CH-(CH_3)-COOH), 4.24 (m, 3H, C*H*-(CH_3)-Ala), 6.60 (dd, 3H, *J* = 6.0, H-Ph6), 6.72 (dd, 3H, *J* = 6.0, H-Ph5), 6.84 (t, 3H, *J* = 6.0, H-Ph4), 7.88 (d, 3H, *J* = 8.0, H-Ph3), 8.02, 8.10 (2 d, 3H, *J* = 2.0, H-Py6), 8.30 (dd, 3H, *J* = 9.0, H-Py4), 8.35 (dd, 3H, *J* = 9.0, *J* = 2.0, H-Py3), 9.0 (m, 3H, NH), ^{13}C NMR (DMSO) δ 16.7 (C-A3), 48.3 (C-A1), 118.5 (C-Py3), 120.4 (C-Ph4), 125.7 (C-Ph3), 130.6 (C-Py5), 136.1 (C-Py4), 136.7 (C-Ph6), 143.0 (C-Ph2), 149.2 (C-Py6), 162.3 (C-Ph1), 163.7 (C-PyCO), 168.5 (C-Py2), 174.6 (C-ACOOH), IR (neat) 3323 (w), 2927 (w), 2844 (w), 1624 (s), 1573 (s), 1475 (m), 1448 (m), 1309 (m), 1242 (m), 1087 (m), 732 (vs) cm^{-1}, MALDI-TOF MS (dithranol) $[M]^+$ Calcd. for: 1000, Found: 1000 HRMS (ESI-MS) Calcd. for: $C_{45}H_{39}IrN_6O_9$ $[M]^+$ 1000.2411, Found: 1000.2451 UV–vis: λ_{abs} 402 nm, λ_{abs} 480 nm, λ_{em} = 567 nm, ε_{402} = 7,697 M^{-1} cm^{-1} ε_{480} = 2,369 M^{-1} cm^{-1} Φ 0.13 (in DMSO).

General Procedure for Hydrogenation/Cleavage of Cbz. The general synthetic route for lysine functionalized iridium(III) complexes is described in Scheme 1. Briefly, the mononuclear iridium(III) complex (0.06 mmol) was dissolved in DMF (10 mL). To this solution was added DCC (0.18 mmol or 3 equiv per free acid), HOBt (0.18 mmol or 3 equiv per free acid), Cbz protected lysine (HCl-salt, 0.018 mmol or 3 equiv per free acid), and DIPEA (0.1 mL), and the reaction mixture was stirred overnight at room temperature. The reaction mixture was concentrated under vacuum, and the crude iridium complex-conjugates were purified by column chromatography (CH_2Cl_2:Aceton 4:1). Afterward the Cbz-protected iridium complex (0.06 mmol) was dissolved in MeOH (25 mL) and 10% Pd/C (50 mg) was added, and the mixture stirred at room temperature under H_2 atm. for 12 h. Afterward the resulting reaction mixture was filtered through Celite 545. The solvent was evaporated to isolate the product as an orange solid in near quantitative yield.

***fac*-(ppy)$_2$(lys-ppy)Ir (17).** Reactants: H_2N-Lys(Cbz)-OMe hydrochloride and complex **8** ^{1}H NMR (DMSO) δ 1.2–1.4 (m, 6H, CH_2-CH_2-CH_2-Lys), 2.73 (m, 2H, H_2N–CH_2-Lys), 3.60, 3.62 (2s, 3H, MeO), 4.33, C*H*-Lys), 6.6–6.9 (m, 9H, H-Ph6,6′,5,5′,4,4′), 7.15 (m, 2H, H-Py4′), 7.53 (2 dd, 2H, *J* = 6.0, H-Py3′), 7.8–8.0 (m, 7H, NH_2, H-Ph3, 3′, H-Py5), 8.00 (2 s, 1H, H-Py6), 8.10 (m, 1H, H-Py6′), 8.26 (2 d, 1H, *J* = 9.0, H-Py4), 8.38, 8.44 (2 d, 1H, *J* = 9.0, H-Py3), 8.98 (br t, 1H, NH), ^{13}C NMR (DMSO) δ 22.5, 24.4, 29.6, 38.4, 53.1, 118.2, 119.4, 120.3, 123.3, 125.1, 125.9, 129.4, 130.5, 136.3, 138.2, 143.3, 144.2, 160.3, 162.9, 165.5, 168.6, 174.1, IR (neat) 3333 (w), 2928 (w), 1732 (s), 1644 (s), 1596 (s), 1579 (s), 1471 (m), 1299 (m), 1159 (m), 1030 (m), 750 (vs), 730 (vs) cm^{-1}, MALDI-TOF MS (dithranol) Calcd. for: $[M+H]^+$ 842, Found: 842 HRMS (ESI-MS) Calcd. for: $C_{41}H_{39}IrN_5O_3$ $[M+H]^+$ 842.2685, Found: 842.2516 UV–vis: λ_{abs} 384 nm, λ_{abs} 484 nm, λ_{em} = 585 nm, ε_{384} = 10,653 M^{-1} cm^{-1} ε_{484} = 2,222 M^{-1} cm^{-1} Φ 0.13 (in DMSO).

***fac*-(ppy)(lys-ppy)$_2$Ir (18).** Reactants: H_2N-Lys(Cbz)-OMe hydrochloride and complex **9** ^{1}H NMR (DMSO) δ 1.2–1.4 (m, 12H, CH_2-CH_2-CH_2-Lys), 2.73 (m, 4H, H_2N–CH_2-Lys), 3.60, 3.62 (2 s, 6H, MeO), 4.33, C*H*-Lys), 6.6–6.9 (m, 9H, H-Ph6,6′,5,5′,4,4′), 7.15 (t, 2H, H-Py4′), 7.53 (m, 2H, H-Py3′), 7.8–8.0 (m, 10H, NH_2, H-Ph3,3′,H-Py5′,6), 8.10 (2 d, 2H, *J* = 9.0 H-Py6′), 8.26 (t, 1H, *J* = 9.0, H-Py4), 8.38, 8.44 (2d, 1H, *J* = 9.0, H-Py3), 8.98 (br t, 1H, NH), ^{13}C NMR (DMSO) δ 22.3, 24.4, 29.7, 38.4, 52.6, 118.2, 119.7, 120.3, 123.3, 125.1, 125.9, 129.6, 130.6, 136.3, 137.9, 143.3, 144.2, 160.3, 163.1, 165.3, 168.6, 173.8, IR (neat) 3322 (w), 2926 (w), 1737 (s), 1625 (s), 1597 (s), 1473 (m), 1224 (m), 1030 (m), 749 (vs), 733 (vs) cm^{-1}, MALDI-TOF MS (dithranol) $[M+2H]^+$ 1029, Found 1029, HRMS (ESI-MS) $C_{49}H_{52}IrN_7O_6$ $[M+H]^+$ Calcd. for: 1028.3690, Found: 1028.3634 UV–vis: λ_{abs} 400 nm, λ_{abs} 485 nm, λ_{em} = 576 nm, ε_{400} = 100,460 M^{-1} cm^{-1} ε_{485} = 2,892 M^{-1} cm^{-1} Φ 0.14 (in DMSO).

***fac*-(lys-ppy)$_3$Ir (19).** Reactants: H_2N-Lys(Cbz)-OMe hydrochloride and complex **10** ^{1}H NMR (DMSO) δ 1.2–1.4 (m, 18H, CH_2-CH_2-CH_2-Lys), 2.70 (m, 6H, H_2N–CH_2-Lys), 3.60 (s, 9H, MeO), 4.20,(m, 3H, C*H*-Lys), 6.55, 6.58 (2d, 3H, *J* = 8.0, H-Ph6), 6.72 (dd, 3H, *J* = 8.0, H-Ph5) 6.85 (dd, 3H, *J* = 8.0, H-Ph4) 7.88 (m, 9H, NH_2-Lys, H-Ph3), 8.07, 8.25 (2 s, 2H, H-Py6), 8.25, 8.32 (2 d, 3H, *J* = 9.0, H-Py4), 8.32, 8.47 (2 d, 3H, *J* = 9.0, H-Py3) 9.0–9.5 (m, 3H, NH), ^{13}C NMR (DMSO) δ 22.1, 26.8, 30.6, 38.8, 52.2, 118.6, 120.5, 125.8, 127.6, 130.4, 136.2, 136.7, 143.6, 148.9, 162.5, 163.9, 168.7, 173.4, IR (neat) 3302 (w), 2927 (w), 2851 (w), 1732 (s), 1633 (s), 1597 (s), 1476 (m), 1225 (m), 1029 (m), 734 (vs) cm^{-1}, MALDI-TOF MS (dithranol) $[M+2H]^+$ Calcd. for: 1215, Found 1215 HRMS (ESI-MS) Calcd. for: $C_{49}H_{52}IrN_7O_6$ $[M+H]^+$ 1214.4696, Found: 1214.4962, UV–vis: λ_{abs} 402 nm, λ_{abs} 484 nm, λ_{em} = 567 nm, ε_{402} = 10,504 M^{-1} cm^{-1} ε_{484} = 3,157 M^{-1} cm^{-1}Φ 0.15 (in DMSO).

Calculated log D (Clog *D*) Values. ChemDraw structures were copied into the structure builder on the Web site http://intro.bio.umb.edu/111-112/OLLM/111F98/newclogp.html. The calculated log of the distribution coefficient (Clog *D*) at pH 7.4 was obtained via Tools, Partitioning, logD for each complex.

Cell Culture. The murine breast cancer cell line 4T1 (kindly provided by Dr. Olaf van Tellingen (NKI/AvL, Amsterdam, The Netherlands) was maintained in Gibco's minimum essential medium (MEM) enriched with 10% fetal bovine serum, 5 mL Penicillin/Streptomycin (10000 units/mL Penicillin/10000 μg/mL Streptomycin), 5 mL L-glutamine, 5 mL nonessential amino acids, 5 mL sodium pyruvate, and 5 mL MEM vitamin solution (all Life Technologies Inc., Breda, The Netherlands). Cells were kept under standard culture conditions.

Flow Cytometry. Freshly cultured 4T1 cells were trypsinized, washed with 0.1% bovine serum albumin in phosphate buffered saline (0.1% BSA/PBS), and then incubated for 1 h at room temperature with the synthesized compound **11**–**19** (0.1 μM) in 0.1% BSA/PBS. Following incubation, cells were washed with 0.1% BSA/PBS, and 5 min prior to analysis, propidium iodide (PI; 1:10000; BD Biosciences) was added to distinguish living from dead cells. After staining, cells

were analyzed using a BD LSRII Special Order System (excitation 355 nm; emission filter 655/8 nm; BD Biosciences). Data was analyzed using FACSDiva Software version 6.1.2 (BD Biosciences).

Confocal Microscopy Analysis. Prior to the start of each experiment, 1.0×10^5 4T1 cells were seeded on coverslips (⌀ 24 mm; Karl Heicht GmbH&Co, Sondheim, Germany). After 24−48 h (80% confluency), the old medium was substituted with fresh culture medium containing 10 μM complex in 0.3% DMSO/cell culture medium and incubated for 1 h at 4 or 37 °C. To visualize the nucleus, lysosomes or endosomes, cells were incubated for 10 min at 37 °C with DAPI (1:1000; Roche, Woerden, The Netherlands), Transferrin conjugate Alexa fluor 647 (1:1000; Invitrogen, Bleiswijk, The Netherlands) or Lysotracker Yellow HCK-123 (1:1000; Invitrogen), respectively. Following incubation, cells were placed on ice and washed three times with icecold PBS. Then images were taken (magnification 630×) and analyzed using a Leica TSC-SP2-AOBS Live confocal microscope (Leica Microsystems Heidelberg GmbH, Mannheim, Germany) equipped with Leica confocal software (Leica Microsystems Heidelberg GmbH). Luminescence emission of the iridium(III) complexes **17**, **18**, and **19** was collected from 580 to 640 nm (excitation at 405 nm), whereas the nucleus was visualized using DAPI (emission collected from 445 to 485 nm; excitation at 405 nm). Lysotracker was used to visualize the lysosomes (emission collected from 510 to 550 nm; excitation at 488 nm) and endosomes could be imaged using transferrin conjugate (emission collected from 650 to 680 nm: excitation at 633 nm).

RESULTS AND DISCUSSION

Synthesis of Mononuclear Iridium Complexes. The iridium(III) complexes **4**, **5**, and **7** were synthesized with the ligand **2**, mppy. The synthesis of **2** deviates from the synthetic route described by Tanaka et al. as we performed a Suzuki coupling with 6-bromo-pyridine-3-carboxylic acid instead of methyl 6-chloro-pyridine-3-carboxylate.[24] First, phenylboronic acid is coupled to 6-bromo-pyridine-3-carboxylic acid in the presence of $[Pd(PPh_3)_4]$ and Na_2CO_3 (Suzuki coupling) leading to the formation of 2-phenyl-5-carboxypyridine in a 90% yield.[25] The so-obtained product was then esterified by $MeOH/H_2SO_4$, the formed methyl ester was isolated in a yield of 90%. The NMR-spectrum of the formed compound **2** was in accordance to that previously reported.[24]

The reaction of the dichloro bridged dimer $[(ppy)_2Ir(\mu\text{-}Cl)_2Ir(ppy)_2]$ **1** with the mppy ligand **2** in the presence of silver triflate[26] resulted in a mixture of four mononuclear iridium(III) complexes. This result implies that ligand exchange reactions took place under these experimental conditions leading to the formation of *fac*-$[Ir(ppy)_3]$ (**3**), the *fac*-$[Ir(ppy)_2mppy]$ (**4**), and *fac*-$[Ir(ppy)mppy_2]$ (**5**). The *fac*-$[Ir(ppy)mppy_2]$ (**5**) is the major product (20%), then *fac*-$[Ir(ppy)_2mppy]$ (**4**) (15%), and finally *fac*-$[Ir(ppy)_3]$ (**3**) (5%, see Scheme 2). As described recently,[27] a small amount of *fac*-$[Ir(mppy)_3]$ (**7**) was also formed, but even after prolonged reaction times the ratio of the product did not change. TLC-monitoring during the reaction reveiled that *fac*-$[Ir(ppy)_2mppy]$ (**4**) was formed first, then *fac*-$[Ir(ppy)mppy_2]$ **5** and *fac*-$[Ir(ppy)_3]$ **3**, and finally a small amount of *fac*-$[Ir(mppy)_3]$ (**7**) could be detected in the reaction mixture. Over time, the amount of *fac*-$[Ir(ppy)mppy_2]$ (**5**) increased and that of *fac*-$[Ir(ppy)_2mppy]$ (**4**) decreased, also indicating a form of ligand exchange/scrambling. It is also possible to synthesize **4** and **5** upon reaction of the dichloro bridged dimer $[(mppy)_2Ir(\mu\text{-}Cl)_2Ir(mppy)_2]$ (**6**) with the ppy ligand. In that case, after 6 h of reaction time, the major product is also *fac*-$[Ir(ppy)mppy_2]$ (**5**) (25%), then *fac*-$[Ir(ppy)_2mppy]$ (**4**) (10%), and finally *fac*-$[Ir(ppy)_3]$ (**3**) together with some traces of *fac*-$[Ir(mppy)_3]$ (**7**). For the formation of *fac*-$[Ir(mppy)_3]$ (**7**) the dichloro bridged dimer $[(mppy)_2Ir(\mu\text{-}Cl)_2Ir(mppy)_2]$ (**6**) was complexed with the mppy ligand **2** in the presence of silver triflate, leading to the formation of the mononuclear iridium complex *fac*-$[Ir(mppy)_3]$ (**7**) in 45% yield (see Scheme 3).

Scheme 2. Synthesis of Complexes 4 and 5

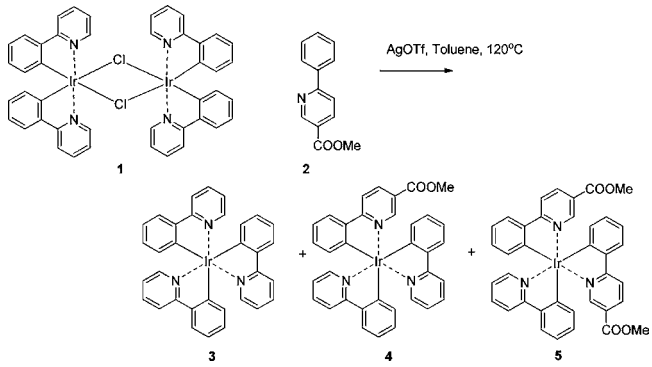

Scheme 3. Synthesis of Complex 7

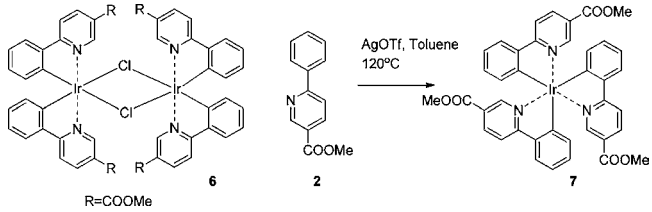

Changing the symmetry of the complex going from the simple spectrum of **3** with C_3 symmetry, to the more complex spectra of **4** and **5** with C_1 symmetry, and finally back to compound **7** with C_3 symmetry immediately has its effect on the complexity of the NMR-spectra (Figure 1). Most characteristic is the dissapearance of Py5, observed in **3** at 7.1 ppm and corresponding to the three Py5 protons in the three identical ppy ligands. In **4** two Py5 signals are observed, corresponding to those of the two ppy ligands that now are inequivalent because of the introduction of the mppy ligand on the iridium and in which a methyl ester is present on the Py5 position. In **5** only one Py5 proton signal is observed, corresponding to the one of the single ppy ligand present in the complex, and in **7** all ppy ligands are substituted by mppy ligands and no Py5 signal is observed. Similar trends in peak shifts and change of peak pattern is observed for other protons. The analysis of the NMR-spectra of the iridium(III) complexes has also been used to determine the ligand configuration of the complexes, either facial (*fac*) or meridonial (*mer*).[28] A *fac* isomer of a homoleptic complex would have all three phenyl ligands on the same face of the molecule, trans to a pyridyl nitrogen, with C_3 symmetry. From the spectrum of compound **7** it can be concluded that the configuration is *fac*, because the 1D-NMR-spectrum gives evidence of the formation of a C_3 symmetric complex, instead of the more complicated pattern that would be obtained for a *mer* complex, with C_1 symmetry. Also it can be concluded that ligand scrambling has no influence on the configuration, there all complexes obtained are *fac*.

After formation of the iridium(III) complexes, the methyl esters were hydrolyzed by LiOH in THF/water, acidification by 1 N HCl resulted in an orange precipitate.[29] The amino acids

dx.doi.org/10.1021/ic201860s | Inorg. Chem. 2012, 51, 2105−2114

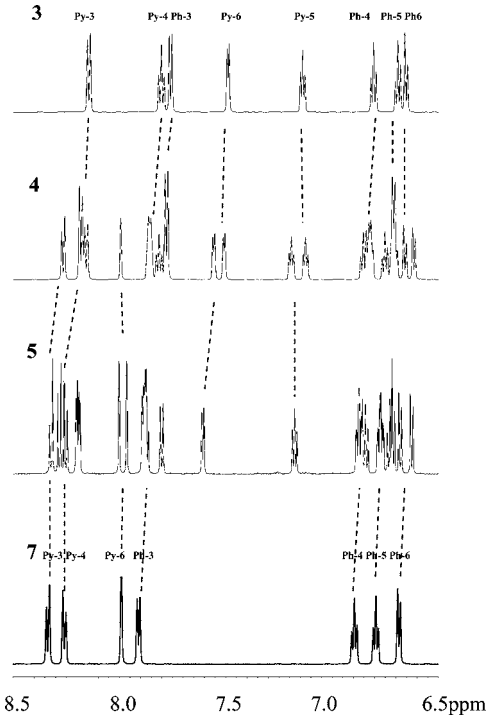

Figure 1. ^{1}H NMR-Spectra (DMSO-d_6) of mono-, bis- and tris(ester) substituted Ir(ppy)$_3$ complexes **4**, **5**, and **7** compared with *fac*-[Ir(ppy)$_3$] **3**.

were coupled to the iridium(III) complexes by standard peptide chemistry coupling procedures (DCC, HOBt, DIPEA, DMF), and directly after purification, the methyl esters were cleaved under the above-reported conditions. The amino acid conjugated complexes were obtained with high purity in near quantitative yields. As a starting-point for the synthesis of these amino acid conjugated iridium(III) complexes, we started with the simplest amino acid glycine; this was followed by alanine, a chiral amino acid yielding diastereomeric complexes, as can be observed by NMR-spectroscopy. Finally the complexes were conjugated to lysine. In aqueous solution at neutral pH, lysine substituents yield the iridium(III) complexes with a positive charge, while glycine and alanine give negatively charged molecules.

The iridium(III) complexes **3**, **4**, **5**, **7**, **13**, **16**, and **19** were characterized using ^{1}H and ^{13}C homo- and heteronuclear NMR experiments. The integration of the signals in the 1D spectra of the complexes showed in all cases the expected number of protons, but severe overlap of peaks in some case complicated unambiguous assignement. The proton signals were assigned to their position in the bicyclic system of the ligand by Correlation Spectroscopy (COSY), Heteronuclear Multiple Quantum Coherence (HC-HMQC), and Heteronuclear Multiple Bond Correlation (HC-HMBC) spectra. HC-HMQC experiments were used to assign the carbon signals to the corresponding proton signals, while assignment of the quaternary carbons and the bridgeheads of the phenyl-pyridine ligands was done by HC-HMBC experiments. Typical and representative 2D NMR spectra of the amino acid conjugated iridium(III) complex **13** are shown in Figures 2 and 3. From the COSY spectra of **13**, the Ph-6,5,4 and 3 protons at 6.60, 6.72, 6.84, and 7.88 ppm are readily assigned, and likewise the pyridine 6 and overlapping 4 and 3 protons, at 8.05 and 8.30 ppm, respectively. Quarternary carbons were assigned from HC-HMBC/HC-HMQC analyses

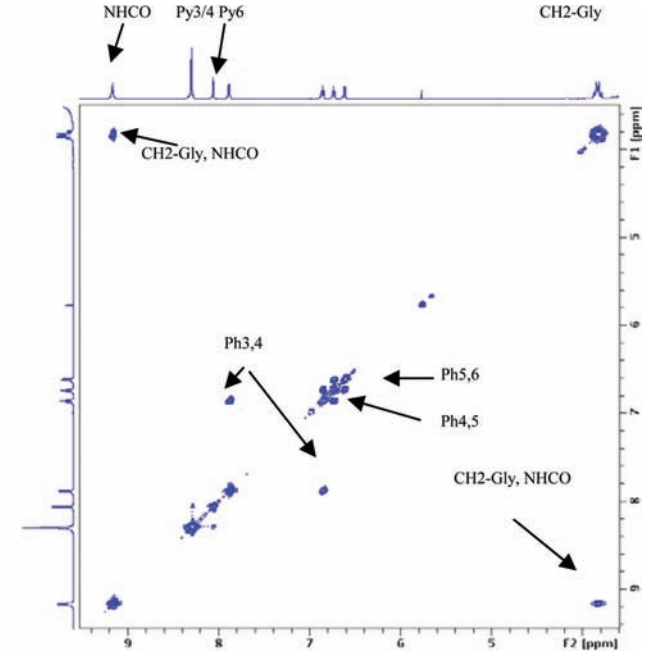

Figure 2. HH−COSY spectrum (DMSO) of Ir(ppy)$_3$ complex conjugated with a glycine on each ppy ligand (**13**).

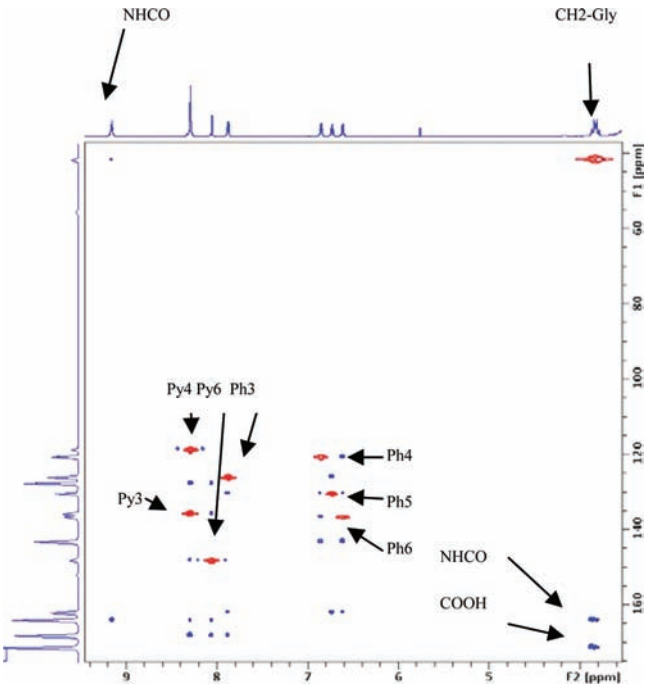

Figure 3. HMBC(blue)/HMQC(red)-spectrum (DMSO) of Ir(ppy)$_3$ complex conjugated with a glycine on each ppy ligand (**13**).

(Figure 3): through correlation with the CH_2 and NH from the glycine the position of the carboxylic acid can be unambiguously assigned at 171.6, and hence the amide at 163.7. Other quarternary carbons are found at 168.5 (Py-2), 143.0 (Ph-2), and 127.4 (Py-5) ppm.

In Figure 4, the NMR-spectra of the amino acid conjugated iridium(III) complexes **13**, **16**, and **19** are shown together for illustrating the spectral changes due to the formation of diastereomers in the latter two complexes. Upon conjugating the Ir(ppy)$_3$ core, consisting of two enantiomeric forms Λ and

dx.doi.org/10.1021/ic201860s | *Inorg. Chem.* 2012, 51, 2105−2114

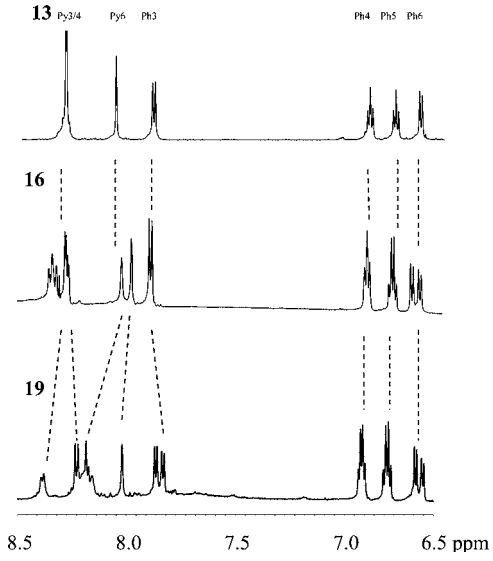

Figure 4. Upfield (aromatic) region of the ^{1}H NMR spectra (DMSO) of tris-substituted Ir(ppy)$_3$ complexes conjugated with glycine (**13**), alanine (**16**), and lysine (**19**). The doubling of peaks due to the formations of diastereomers in **16** and **19** is most evident for the Ph3, Ph6, and Py6 protons.

Δ,[30] with a homochiral amino acid (L-alanine or L-lysine) instead of an achiral L-glycine, the pattern of the peaks in the spectrum changes dramatically, giving evidence for the two stereoisomeric forms of the iridium(III)-complexes **16** and **19**. With respect to the spectrum of **13**, the number of peaks for the Py3, Py4, and Py6 protons is doubled, as well as the peaks of Ph3, Ph4, Ph5, and Ph6. This is most evident for the Ph3 and Ph6 protons, which both show a doublet when conjugated to glycine (**13**), but show both two doublets when conjugated to lysine (**19**). The peak pattern of the Ph4 and Ph5 also doubles, but the changes in chemical shift are small, and the multiplets overlap severely. Also illustrative is the Py6 peak, observed as a clear singlet for **13**, but two singlets are observed in the spectra of **16** and **19**. For the lysine conjugated complex **19** the difference observed for the diastereotopic protons (up to ~0.2 ppm) is significantly bigger than that observed for the alanine conjugated iridium(III) complex **16**, which can be attributed to the larger functional group on the lysine and the consequential greater steric constraint with the tris(ppy) unit.

The quantitative cellular uptake in 4T1 cells of the iridium(III) complexes **11**−**19** was compared using flow cytometry (Figure 5). Interestingly, the monosubstituted complexes **11**, **14**, and **17**, gave a remarkable 20-fold higher cellular uptake than the corresponding bis- and tris- substituted analogues (Figure 5). This difference is most likely because the monosubstituted iridium(III) complexes are more hydrophobic, and this generally favors the uptake.[31,32] To quantify the hydrophobicity of complexes **11**−**19**, log *P* or Clog *D* values were determined. Because of poor solubility in both the octanol and water layer (solutions stay turbid and the complexes act as surfactants), the log *P* values could not be measured and were therefore calculated at pH 7.4 (Table 1). These values clearly illustrate that the monosubstituted complexes are hydrophobic and the bis- and tri- substituted complexes are hydrophilic, suggesting that hydrophobicity is important for the cellular uptake of the dye. The Clog *D* values also show that the lysine conjugated complexes are slightly more hydrophobic than the glycine and alanine derivatives.

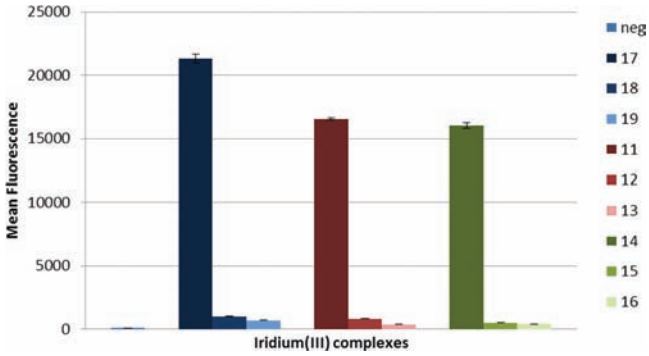

Figure 5. Cellular uptake of complexes **11**−**19** (10 μM in PBS) in 4T1 cells after 1 h incubation.

Table 1. Calculated log D (Clog *D*) Values at pH 7.4

compound	Clog *D*
11	2.05
12	−3.03
13	−8.12
14	2.61
15	−1.92
16	−6.45
17	3.18
18	−0.76
19	−4.70

This difference could explain why lysine complexes **17**−**19** display relatively higher uptake with respect to the corresponding alanine or glycine derivative. However, this relatively high uptake could also be caused by the positive charge at the lysine side chain, since positive charges commonly enhance uptake (e.g., cell penetrating peptides). The amphiphilic character of the iridium complexes, with a hydrophobic core and hydrophilic substituents, makes it possible to tune the complexes with concern to their lipophilicity, and therefore, cellular uptake.[33] The monosubstituted iridium(III) complexes are significantly more hydrophobic and possibly this favors the uptake.

Because of their relatively high uptake, the cellular distribution of complex **17**, **18**, and **19** was studied in more detail using confocal microscopy (Figure 6). After incubating the cells with 10 μM **17**−**19** for 1 h at 4 and 37 °C, different types and intensities of cell staining were observed.[34] Upon incubation of cells at 4 °C, cellular metabolism is shut down and therefore, a limited amount of cellular dye uptake is expected under these conditions (nonspecific uptake through the membrane), whereas at 37 °C cellular metabolism is fully functional and more specific dye uptake in the cell can be expected, for example, via membrane vesicles. At 4 °C, slight incorporation of complex **17** (Figure 6A) occurred; during the imaging procedure the cells were maintained at 37 °C, which resulted in stronger uptake of the dye. This uptake seems to occur through the lysosomes as a similar staining pattern was observed when 4T1 cells were incubated with Lysotracker (Figure 6B). Very little to no staining was observed when 4T1 cells were incubated at 4 °C with complex **18** or **19**, respectively (Figure 6A). On the other hand, incubation of 4T1 cells with complex **17**, **18**, or **19** at 37 °C resulted in significantly more intense staining. In contrast to complex **18** and **19**, strong staining throughout the cells was observed for complex **17** (Figure 6A), except in the nucleus (compared to nucleus staining in Figure 6B). For complex **18** and **19**, the

dx.doi.org/10.1021/ic201860s | *Inorg. Chem.* 2012, 51, 2105−2114

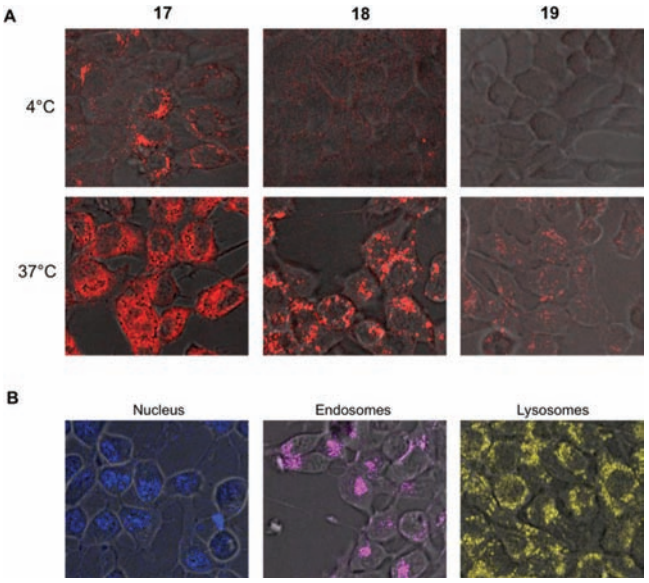

Figure 6. Confocal microscopy images of the cellular distribution of the various lysine substituted iridium(III) complexes. (A) Difference in distribution of the number of lysine residues from left to right: mono- (**17**), bis- (**18**), and tris- (**19**) substituted complexes. Cells were incubated for 1 h at 4 °C (top row) or 37 °C (bottom row) with 10 μM complex in 0.3% DMSO/cell culture medium. Cell transmission images were overlaid with the luminescence image. (B) Various cells structures: nucleus (staining with DAPI), endosomes (staining with transferrin conjugate), and lysosomes (staining with Lysotracker). Cell transmission images were overlaid with the luminescence image.

staining patterns again suggested that the complexes incorporate through the lysosomes (Figure 6B). In vitro spectroscopic measurements of the luminescence spectra all showed a maximum emission around 580 nm (see Table 2), proving

Table 2. Photophysical Data of Complexes 11−19

compound	$\lambda_{abs/nm}$ (10^3 M^{-1} cm^{-1})	$\lambda_{em/nm}$ λ_{exc} 480 nm	Φ
11	382(9,096), 483(1,187)	579	0.12
12	401(7,402), 482(1,858)	576	0.13
13	405(8,443), 485(2,013)	564	0.11
14	382(7,152), 484(1,444)	579	0.11
15	401(6,554), 483(2,005)	570	0.12
16	402(7,697), 480(2,369)	567	0.13
17	384(10,653), 484(2,222)	585	0.13
18	400(10,460), 485(2,892)	576	0.14
19	402(10,504), 484(3,157)	567	0.15

the intracellular luminescence was indeed caused by the respective iridium(III) complexes. Similar to Fernandez-Moreira et al.,[35] under all conditions tested, no nuclear staining was observed (Figure 6B). However, as shown in Supporting Information, Figure S13, we found nuclear staining of complex **19** when we used a higher percentage (1%) of DMSO during incubation, as observed by others.[21,36] In the bright field images of the stained cells a dark contrast was observed at locations that had a high luminescence intensity, that is, the nucleoli. This increase in light attenuation corroborates with the high local concentration of iridium(III) complexes as observed from the luminescence images. Reference staining for the nucleus, endosomes, and lysosomes were obtained in separate cell-culture samples of the same 4T1 cell line (Figure 6B).

From the quantum yield, shown in Table 2, it can also be concluded that the fully cyclometalated iridium(III) complexes maintain their relatively high luminescence in solution/cells. Moreover, the quantum yield of the complexes lies within the same range (0.11−0.15) and for this reason the cellular uptake determined by flow cytometry of the different amino acid conjugated iridium(III) complexes can be compared.

Flow cytometric analysis (common PI uptake assay; Figure 7) was used to to determine the influence of the different

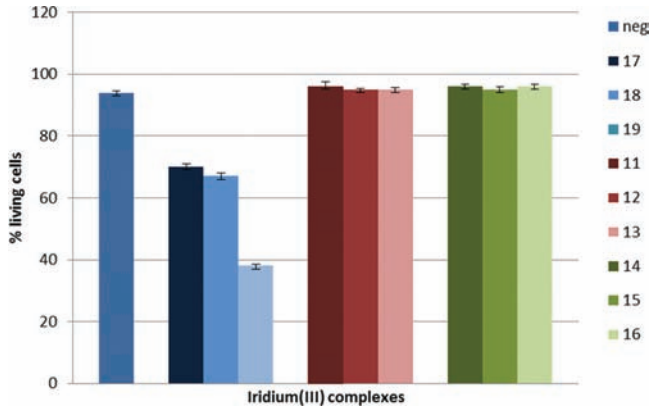

Figure 7. Cell viability after treatment of 4T1 cells with complexes **11**−**19**.

iridium(III) complexes have on the tumor cells. Only the lysine functionalized complexes showed reduced cell viability. Viability further decreased with the number of lysine substituents from 71% and 70% to 39%, from the mono and bis, respectively, to the tris functionalized complex. This observation runs in parallel with the increasing positive charges on complexes **17**, **18**, and **19**.

CONCLUSION

In conclusion, a series of nine iridium(III) complexes with the archetypical parent $Ir(ppy)_3$ as core unit, has been synthesized, fully characterized by 1D and 2D NMR spectroscopy, and the cellular uptake pattern has been investigated. The number (mono-, bis-, tris-) and type (glycine, alanine, lysine) of amino acids influence both the cellular uptake and, to a lesser extent, intracellular localization of the complex. All three monosubstituted iridium(III) complexes gave a remarkably higher cellular uptake than the bis- and tris- substituted complexes. Iridium(III) complexes conjugated to lysine show in general a higher uptake with respect to the correspondingly substituted glycine and alanine derivatives. Moreover, the lysine derivatives show an increased cellular toxicity. The high quantum yield of the dyes, combined with their relative high cellular uptake, makes the fully cyclometalated tris(ppy) iridium(III) complexes a promising class of luminescent labels for (bio)imaging agents, allowing finetuning of the properties of the complexes. Further investigations are currently focused on integration of amino-acid functionalized iridium(III) complexes in (automated) peptide synthesis and biomarker specific targeting agents.

ASSOCIATED CONTENT

Supporting Information

The aromatic region of HH-COSY, HC-HMBC and HC-HMQC spectra of compounds **3**, **4**, **5**, and **7**. Additional

dx.doi.org/10.1021/ic201860s | Inorg. Chem. 2012, 51, 2105−2114

confocal images of compound **19**. This material is available free of charge via the Internet at http://pubs.acs.org.

AUTHOR INFORMATION

Corresponding Author

*E-mail: a.h.velders@utwente.nl; Aldrik.Velders@wur.nl.

Notes

The authors declare no competing financial interest.

ACKNOWLEDGMENTS

The authors would like to thank Tieme Stevens, Bianca Snellink-Ruël, Frank van Diepen, and Anita Pfauth for their technical support.

REFERENCES

(1) Pascu, S. I.; Waghorn, P. A.; Conry, T. D.; Lin, B.; Betts, H. M.; Dilworth, J. R.; Sim, R. B.; Churchill, G. C.; Aigbirhio, F. I.; Warren, J. E. *Dalton Trans.* **2008**, *37*, 2017−2010.

(2) Pascu, S. I.; Waghorn, P. A.; Conry, T. D.; Betts, H. M.; Dilworth, J. R.; Churchill, G. C.; Pokrovska, T.; Christlieb, M.; Aigbirhio, F. I.; Warren, J. E. *Dalton Trans.* **2007**, *36*, 4988−4997.

(3) (a) Fernandez-Moreira, V.; Thorp-Greenwood, F. L.; Coogan, M. P. *Chem Commun.* **2010**, *46*, 186−202. (b) Chen, Z.; Bian, Z.; Huang, C. *Adv. Mater.* **2010**, *22*, 1534−1539. (c) Lo, K. K.-W.; Louie, M.-W.; Zhang, K. Y. *Coord. Chem. Rev.* **2010**, *254*, 2603−2622. (d) Lo, K. K.-W.; Li, S. P.-Y.; Zhang, K. Y. *New J. Chem.* **2011**, *35*, 265−287. (e) Pucket, C. A.; Ernst, R. J.; Barton, J. K. *Dalton Trans.* **2010**, *39*, 1159−1170. (f) Ruggi, A.; Reinhoudt, D. N.; Velders, A. H. Biomedical applications of metal-containing luminophores. In *Bioinorganic Medicinal Chemistry*; Wiley: New York, 2011; pp 397−421; (g) Ruggi, A.; Van Leeuwen, F. W. B.; Velders, A. H. *Coord. Chem. Rev.* **2011**, *255*, 2542−2554.

(4) Ma, B.; Djurovich, P. I.; Thompson, M. E. *Coord. Chem. Rev.* **2005**, *249*, 1501−1510.

(5) Stephens, D. J.; Allen, V. J. *Science* **2003**, *300*, 82−86.

(6) (a) Zhang, M.; Yu, M. X.; Li, F. Y.; Zhu, M. W.; Li, M. Y.; Gao, Y. H.; Li, L.; Liu, Z. Q.; Zhang, D. Q.; Yi, T.; Huang, C. H. *J. Am. Chem. Soc.* **2007**, *129*, 10322−10323. (b) Wu, J. C.; Yi, T.; Zou, Y.; Xia, Q.; Shu, T. M.; Liu, F.; Yang, Y. H.; Li, F. Y.; Chen, Z.; Zhou, Z. G.; Huang, C. H. *J. Mater. Chem.* **2009**, *19*, 3971−3978. (c) Chen, Z. G.; Chen, H. L.; Hu, H.; Yu, M. X.; Li, F. Y.; Zhang, Q.; Zhou, Z. G.; Yi, T.; Huang, C. H. *J. Am. Chem. Soc.* **2008**, *19*, 3971−3972.

(7) Yu, M. X.; Li, F. Y.; Chen, Z. G.; Hu, H.; Zhan, C.; Yang, H.; Huang, C. H. *Anal. Chem.* **2009**, *81*, 930−935.

(8) (a) Haugland, R. P. *A Guide to Fluorescent Probes and Labbeling Technologies*, 10th ed.; Molecular Probes: Eugene, OR, 2005. (b) Kuil, J.; Steunenberg, P.; Chin, P. T. K.; Oldenburg, J.; Jalink, K.; Velders, A. H.; Van Leeuwen, F. W. B. *ChemBioChem* **2011**, *12*, 1897−1903.

(9) (a) Amoroso, A. J.; Coogan, M. P.; Dunne, J. E.; Fernandez-Moreira, V.; Hess, J. B.; Hayes, A. J.; Lloyd, D.; Millet, C.; Pope, S. J. A.; Williams, C. *Chem Commun.* **2007**, *43*, 3066−3068. (b) Murphy, L.; Congreve, A.; Palsson, L.-O.; Williams, J. A. G. *Chem Commun.* **2010**, *46*, 8743−8745.

(10) (a) Lamansky, S.; Djurovich, P.; Murphy, D.; Abdel-Razzag, F.; Lee, H. E.; Adachi, C.; Burrows, P. E.; Forrest, S. R.; Thompson, M. E. *J. Am. Chem. Soc.* **2001**, *123*, 4304−4312. (b) You, Y. M.; Park, S. Y. *J. Am. Chem. Soc.* **2005**, *127*, 12438−12439. (c) Holder, E.; Langeveld, B. M. W.; Schubert, U. S. *Adv. Mater.* **2005**, *17*, 1109−1121.

(11) (a) Gao, R. M.; Ho, D. G.; Hernandez, B.; Selke, M.; Murphy, D.; Djurovich, P. I.; Thompson, M. E. *J. Am. Chem. Soc.* **2002**, *124*, 14828−14829. (b) Xie, Z.; Ma, L.; DeKrafft, K. E.; Jin, A.; Lin, W. *J. Am. Chem. Soc.* **2010**, *132*, 922−923. (c) Chen, H.; Zhao, Q.; Wu, Y.; Li, F.; Yang, H.; Yi, T.; Huang, C. *Inorg. Chem.* **2007**, *46*, 11075−11081.

(12) Bolink, H. J.; Capelli, L.; Coronado, E.; Grätzel, M.; Orti, E.; Costa, R. D.; Viruela, P. M.; Nazeeruddin, M. K. *J. Am. Chem. Soc.* **2006**, *128*, 14786−14787.

(13) (a) Chen, F. F.; Bian, Z. Q.; Liu, Z. W.; Nie, D. B.; Chen, Z. Q.; Huang, C. H. *Inorg. Chem.* **2008**, *47*, 2507−2513. (b) Chen, F. F.; Bian, Z. Q.; Lou, B.; Ma, E.; Liu, Z. W.; Nie, D. B.; Chen, Z. Q.; Bian, J.; Chen, Z. N.; Huang, C. H. *Dalton Trans.* **2008**, *37*, 5577−5578.

(14) DeRosa, M. C.; Hodgson, D. J.; Enright, G. D.; Dawson, B.; Evans, C. E. B.; Crutchley, R. J. *J. Am. Chem. Soc.* **2004**, *126*, 7619−7626.

(15) Lo, K. K.-W.; P.-K. Lee, P.-K.; Lau, J. S.-Y. *Organometallics* **2008**, *13*, 2998−3006.

(16) Yu, M.; Zhao, Q.; Shi, L.; Li, F.; Zhao, Z.; Yang, H.; Yia, T.; Huang, C. *Chem. Commun.* **2008**, *44*, 2115−2117.

(17) Zhao, Q.; Yu, M.; Shi, L.; Lui, S.; Li, C.; Shi, M.; Zhou, Z.; Huang, C.; Li, H. *Organometallics* **2010**, *29*, 1085−1091.

(18) Kim, J. I.; Shin, I.-S.; Kim, H.; Lee, J.-K. *J. Am. Chem. Soc.* **2005**, *127*, 1614−1615.

(19) Zhang, K. Y.; Lo, K. K.-W. *Inorg. Chem.* **2009**, *48*, 6011−6025.

(20) (a) Colombo, M. G.; Brunold, T. C.; Riedener, T.; Gudel, H. U.; Fortsch, M.; Burgi, H.-B. *Inorg. Chem.* **1994**, *33*, 545−550. (b) Lamansky, S.; Djurovich, P.; Murphy, D.; Abdel-Razzaq, F.; Kwong, R.; Tsyba, I.; Bortz, M.; Mui, B.; Bau, R.; Thompson, M. E. *Inorg. Chem.* **2001**, *40*, 1704−1711.

(21) Li, C.; Yu, M.; Sun, Y.; Wu, Y.; Huang, C.; Li, F. *J. Am. Chem. Soc.* **2011**, *123*, 11231−11239.

(22) Montalti, M.; Credi, A.; Prodi, L.; Gandolfi, M. T. *Handbook of Photochemistry*; CRC Press: Boca Raton, FL, 2006.

(23) (a) Sprouse, S.; King, K. A.; Spellane, P. J.; Watts, R. J. *J. Am. Chem. Soc.* **1984**, *106*, 6647−6653. (b) Baranoff, E.; Suarez, S.; Bugnon, P.; Bolink, H. J.; Klein, C.; Scopelliti, R.; Zuppiroli, L.; Grätzel, M.; Nazeeruddin, Md. K. *ChemSusChem* **2009**, *2*, 305−308. (c) Holder, E.; Marin, V.; Aleev, A.; Schubert, U. S. *J. Polym. Sci., Part A: Polym. Chem.* **2005**, *43*, 2765−2776. (d) Garces, F. O.; King, K. A.; Watts, R. J. *Inorg. Chem.* **1988**, *27*, 3464−3471. (e) Kappaun, S.; Eder, S.; Sax, S.; Mereiter, K.; List, E. J. W.; Slugovc. *Eur. J. Inorg. Chem.* **2007**, 4207−4215.

(24) Tanaka, A.; Terasawa, T.; Hagihara, H.; Sakuma, Y.; Ishibe, N.; Sawada, M.; Takasugi, H.; Tanaka, H. *J. Med. Chem.* **1998**, *41*, 2390−2410.

(25) (a) Meier, P.; Legraverant, S.; Muller, S.; Schaub, J. *Synthesis* **2003**, *3*, 551−554. (b) Zeng, X.; Batsanov, A. S.; Bryce, M. R. *J. Org. Chem.* **2006**, *71*, 9589−9594.

(26) (a) Beeby, A.; Bettington, S.; Samuel, I. D. W.; Wang, Z. *J. Mater. Chem.* **2003**, *13*, 80−83. (b) Wang, X.-Y.; Kimyonok, A.; Weck, M. *Chem Commun.* **2006**, *42*, 3933−3935.

(27) Sato, H.; Tamura, K.; Taniguchi, M.; Yamagishi, A. *New J. Chem.* **2010**, *34*, 617−622.

(28) Brisig, B.; Constable, E. C.; Housecroft, C. E. *New J. Chem.* **2007**, *31*, 1437−1447.

(29) Ohkando, J.; Ritsuko, S.; Kato, N. *Chem. Commun.* **2009**, *45*, 6949−6951.

(30) Tamayo, A. B.; Alleyne, B. D.; Djurovich, P. I.; Lamansky, S.; Tsyba, I.; Ho, N. N.; Bau, R.; Thompson, M. E. *J. Am. Chem. Soc.* **2003**, *125*, 7377−7387.

(31) (a) Le, U. A.; Cui, Z. R. *Int. J. Pharm.* **2006**, *312*, 105−112. (b) Abraham, S. A.; Edwards, K.; Karlsson, G.; MacIntosh, S.; Mayer, L. D.; McKenzie, C.; Bally, M. B. *Biochim. Biophys. Acta* **2002**, *1565*, 41−54. (c) Ghezzi, A.; Aceto, M.; Cassino, C.; Gabano, E.; Osella, D. *J. Inorg. Biochem.* **2004**, *98*, 73−78. (d) Berkers, C. R.; Van Leeuwen, F. W. B.; Groothuis, T.; Peperzak, V.; Van Tilburg, E. W.; Borst, J.; Neefjes, J. J.; Oova, H. *Mol. Pharmaceutics* **2007**, *4*, 739−748.

(32) VanBrocklin, H. F.; Liu, A.; Welch, M. J.; O'Neil, J. P.; Katzenellenbogen, J. A. *Steroids* **1994**, *59*, 34−35.

(33) Jiang, W.; Gao, Y.; Sun, Y.; Ding, F.; Xu, Y.; Bian, Z.; Li, F.; Bian, J.; Huang, C. *Inorg. Chem.* **2010**, *49*, 3252−3260.

(34) (a) Kobayashi, T.; Arakawa, Y. *J. Cell Biol.* **1991**, *113*, 235−244. (b) Pagano, R. E.; Martin, O. C.; Kang, H.-C.; Haugland, R. P. *J. Cell Biol.* **1991**, *113*, 1267−1279. (c) Kuil, J.; Buckle, T.; Yuan, H.; Oishi, S.; Fujii, N.; Josephson, L.; Van Leeuwen, F. W. B. *Bioconjugate Chem.* **2011**, *22*, 859−864.

(35) Fernandez-Moreira, V.; Thorp-Greenwood, F. L.; Amoroso, A. J.; Cable, J.; Court, J. B.; gray, V.; Hayes, A. J.; Jenkins, R. L.; Kariuki, B. M.; Lloyd, D.; Millet, C. O.; Williams, C. Ff.; Coogan, M. P. *Org. Biomol. Chem.* **2010**, *8*, 3888−3901.
(36) (a) Botchway, S. W.; Charnley, M.; Haycock, J. W.; Parker, A. W.; Rochester, D. L.; Weinstein, J. A.; Williams, J. A. G. *Proc. Natl. Acad. Sci. U. S. A.* **2008**, *105*, 16071−16076. (b) Kowol, C. R.; Trondl, R.; Arion, V. B.; Jakupec, M. A.; Lichtscheidl, I.; Keppler, B. K. *Dalton Trans.* **2010**, *39*, 704−706. (c) Puckett, C. A.; Barton, J. K. *Bioorg. Med. Chem.* **2010**, *18*, 3564−3569. (d) Zhang, K. Y.; Li, S. P.-Y.; Zhu, N.; Or, I. W.-S.; Cheung, M. S.-H.; Lam, Y.-W.; Lo, K. K.-W. *Inorg. Chem.* **2010**, *49*, 2530−2540.